Cerebrospinal Pulsation Hydrodynamics in a 2D Simulation of Brain Ventricles

N. Masoumi[i]; D. Bastani[ii]; S. Najarian[iii]; F. Farmanzad[iv]; A.M. Seddighi[v]

ABSTRACT

In this article, dynamics of the cerebrospinal fluid (CSF) was studied, using computational fluid dynamics. Using MRI images of two special cases, a 2-dimensional model of the ventricular system was made. CSF velocity and pressure distribution in ventricular system have high importance since the flow pattern of this liquid has an important effect on intracranial pressure, i.e., ICP, which has a key role in treatment of patients suffering from brain trauma. The pulsatile nature of CSF production, which is a result of arterial blood pressure in choroid plexuses, is considered for the first time. Finite element analysis of ventricular area with CFD analyzer software was processed using ADINA 8.2. Pressure distribution in different conditions of CSF production, i.e., constant input flow rate and pulsatile input flow rate, were compared. Comparison between the simulation results and reported experimental data depicted that modeling CSF with pulsatile production nature is more realistic.

KEYWORDS

Cerebrospinal Fluid (CSF), Intracranial pressure (ICP), Aqueduct velocity, Hydrodynamic modeling

1. INTRODUCTION

Human brain floats in a clear and colorless fluid named cerebrospinal fluid (CSF) which flows in brain ventricles and subarachnoid space. One of the most important functions of CSF is to protect the brain tissue from injury as it gets jolted or hit. This fluid is not static and is continually produced in the brain by blood vessels at a rate of about 600 ml/day. Since the skull can only contain 135 to 150 ml of CSF, larger amounts of the fluid are drained primarily into the blood circulation system. So, the pressure inside the skull is directly related to the fluid absorption rate [1].

Determination of CSF Pressure (ICP) is one of the most important parameters in treatment of damaged brains. As ICP has important effects on cerebral perfusion pressure (CPP) and the flexibility of brain tissue, it gives valuable information about blood and CSF circulation in the brain. Along with the mentioned effects, increased brain pressure can avoid blood circulation, leading to anemia or causing disordered fluid circulation in illnesses such as hydrocephalus. This pressure is a function of ventricle shape and size, mechanical properties of surrounded tissue, CSF properties and its flow pattern and finally the blood circulation inside the brain. Hydrodynamic analysis of CSF is of great use in the studies of different insufficiencies which emphasizes the scientific importance and necessity of this investigation.

Conventional CSF hydrodynamics is based on different theoretical methods, mathematical calculations, numerical modeling and analysis of MRI images, one of which is simulation of CSF circulation and brain deformation using finite element methods. Unfortunately complex geometry and different properties of brain tissue

[i] N. Masoumi is with the Department of Chemical and Petroleum Engineering, Sharif University of Technology, Tehran, Iran (e-mail: masoomy@mehr.sharif.edu)

[ii] D. Bastani is with the Department of Chemical and Petroleum Engineering, Sharif University of Technology, Tehran, Iran (e-mail: bastani@sharif.edu)

[iii] S. Najarian is with the Robotic Surgery and Artificial Tactile Sensing Laboratory, Faculty of Biomedical Engineering, Amirkabir University of Technology, Tehran, Iran (email: najarian@aut.ac.ir)

[iv] F. Farmanzad is with the Department of Mechanical Engineering, Iran University of Science and Technology, Tehran, Iran (email: Farmanzad@iust.ac.ir)

[v] A. M. Seddighi is with the Medical Science Department, Shahid Beheshti University, Tehran, Iran (email: Invincible19152@gmail.com)

make this method very difficult to be applied. However, a simple but exact model of brain and its ventricles can be useful for evaluation of CSF hydrodynamics and pressure distribution and is of great help for prediction and treatment of cerebrospinal problems. Due to great advancements of computational capacities and widespread use of software simulation over the last decade, it has become possible to build models on real, albeit simplified anatomical geometries.

Study of CSF flow has been proposed by Ursino et al in 1988 [2]. In the past decade several studies have been done on CSF dynamics using computer simulations. Jacobson et al [3], Loth et al [4] and Kurtcuoglu et al [5] are the investigators who presented models by means of CFD analysis and extracting CSF pressure and velocity information showing that largest pressure drop and velocity happens in aqueduct of Sylvius. The 3-D analyzed geometrical model by Aroussi et al [6, 7] has shown relative pressure and velocity distribution in ventricles. Finite element model done by Gibson et al is another project in this area. 3D geometrical model by Kurtcuoglu and CSF dynamics analysis in special locations including third ventricle and aqueduct is another work of this group. The preference of some research activities is 3D modeling, although only some parts of ventricle system are being modeled (see Table 1).

In all of the mentioned models, surrounded tissue is disregarded for simplicity. According to current investigations [9, 10] CSF is produced as a result of heart beating and vascular pressure and has pulsating nature. This quality of the flow was not applied in any of the mentioned research works, not even in the form of boundary conditions. In this article, in addition to exact modeling of ventricles system from MRI images, exact model of CSF flow hydrodynamics was employed as a result of exact input/output conditions. The results are quantitatively comparable to the experimental observations. The quantitative results of this experiment were compared with experimental observations in order to confirm modeling. In the end, a comparison was done between constant and pulsatile input.

2. MATERIALS AND METHODS

Gathering geometrical information of candidates including ventricles and skull dimensions was done via exact imaging. With the help of T2 scanners suitable accuracy is obtained. Images by T2WI method were clear and ready for analysis. In the next stage, MRI images were entered into drawing environment of CATIA and geometrical boundary of brain tissue and ventricles extracted according to Fig.1. Substituting governing equations and balancing the mass and momentum on fluid flow on ventricles, show CSF flow and intra ventricular pressure (IVP) distribution.

At first, boundaries were determined in two healthy persons (one 21 years old and another 63 years old, both male, see Fig. 1) and 2D geometrical model was constructed. Simplifications were applied to the model after changing the model to a suitable format for ADINA software. CSF was considered as a Newtonian fluid. After applying boundary conditions and determination of input flow as a function of time, fluid dynamics was accessible.

A. GEOMETRICAL MODELING

2D geometrical model was obtained from MRI images in transverse section. The model was saved as IGES format and entered in ADINA 8.2 software. After exiting from fourth ventricle, the CSF enters subarachnoid space. Investigations show that pressure in this region is approximately equal to the pressure inside ventricles [10]. CSF pressure difference in this region and the pressure in vascular sagittal sinus are the main factors in fluid absorption of vascular circulation system. Subarachnoid space is disregarded for simplicity. An output flow from Magendie foramina is considered. Fig.1 shows two 2D geometrical model obtained from MRI images.

B. INPUT, OUTPUT AND BOUNDARY CONDITIONS

The system inlet is the lateral ventricle, above the third ventricle in the choroid plexus location. Input, output and boundary conditions for both cases are as mentioned in table 2. CSF production flow $q_i(t)$ in choroid plexus is defined from equation (1):

$$q_i(t) = q_{bulk} + q_{puls}(t) \tag{1}$$

$$q_{puls}(t) = \alpha\left[\sin\left(\omega t - \frac{\pi}{2}\right) - \frac{1}{2}\cos\left(2\left(\omega t - \frac{\pi}{2}\right)\right)\right] \tag{2}$$

where q_{bulk} is constant production flow of about $0.32\,cm^3/\min$ and $q_{puls}(t)$ is the pulsatile flow which is related to heart beat. Clearly mean periodic flow equals $0.32\,cm^3/\min$.

As the production rate of CSF inside fourth ventricle is negligible (approximately $0.032\,cm^3/\min$) [10], this region is not considered in the simulations. The ventricle wall treated as inflexible for more simplicity of the model. Zero velocity on the wall and zero pressure for the output were set as boundary conditions.

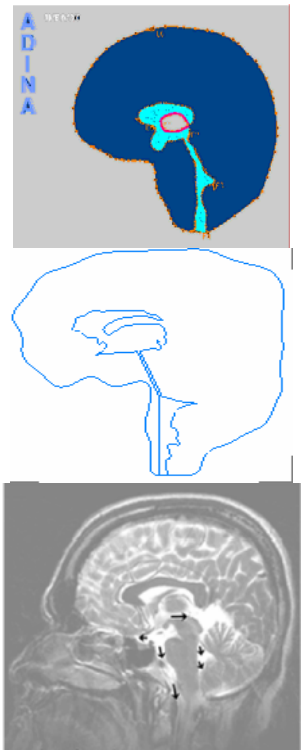

Fig.1: 2D modeling from MRI image.

C. CFD AND FINITE ELEMENTS ANALYSIS

A computational model for predicting CSF motion was used. Equations related to mass and momentum balance were solved by CFD method on mentioned regions. For this purpose, a few parameters were needed. These include fluid viscosity and density that are represented in Table 3. The results of this analysis are CSF velocity and ICP pressure in the ventricles.

In this research, CSF has been considered as a Newtonian viscous fluid. The flow is assumed laminar for more simplifications. Fluid is considered as incompressible, thus density changes are negligible in equations. Since the flow inside the ventricles has a pulsatile nature, the analysis can be considered dynamic for the fluid. The governing equations of continuity and momentum were employed. ADINA 8.2 has been used for the analysis. Fluid model was created in ADINA-F environment as the meshing was done and adjusted by ADINA-M. The size of elements was adjusted in order to prevent divergence. In the mean time, geometrical complexity was preserved for more accuracy. Elements of type "4 nodes quadratic" were used in the mesh.

The amount of optimized elements in the two models was 3060 and 2985 and the number of nodes was 1734 and 1696, respectively. Considering the assumption that the output flow exits from the end surface (Magendie foramina), the input flow was divided on Magendie foramina area of 2mm radius and the velocity at this point was obtained to be equal to $2.5\,{}^{mm}\!/_{\sec}$. Experimental results from CINE method show that the velocity at this point should be in the range of $2-6\,{}^{mm}\!/_{\sec}$ [9-12].

3. RESULTS

The simulation has to go on for one second in order to pass the transient condition. In addition to the geometrical model (2D), elements type and size are the factors which can affect the length of this time. The results of velocity and pressure distribution in CSF circulation system for the first person in both pulsatile and constant input are represented in Fig.2 and Fig.3, respectively. Fig.4 shows this result for the second person with the assumption of pulsatile input. Table 4 and Table 5 compare the results of constant and pulsatile inputs for the two cases with previously published experimental data. According to the results, largest velocity is about $8\,\text{to}\,10\,{}^{mm}\!/_{\sec}$ occurring in aqueduct for the case of pulsatile flow, while the maximum velocity of $4.5\,\text{to}\,8\,{}^{mm}\!/_{\sec}$ occurring for the constant flow model. For both models largest pressure drop was seen in the aqueduct as well with the value of $0.7-1.5\text{Pa}$ for the pulsatile models and $0.3-0.5\text{Pa}$ for the case of constant flow. As mentioned before, the results are based on simplifying assumptions. Neglecting the arachnoid space does not have considerable effect on the results. But considering rigid wall for CSF can lead to results far from reality. The overall results of the models, fluid flow pattern and pressure distribution, are in agreement with CINE-MRI experiments [3, 4, 12, 13]. The results of this article can be a basis for future investigations with more realistic conditions. In addition, the fact that these results are not accessible via medical instruments can help the doctors and give them useful information in the case of diseases that have hydrodynamics agents or drug delivery that need fluid velocity at different points (Fig.5).

4. DISCUSSION

The 3D modeling of the brain is considered to have more realistic results. Unfortunately, construction of such models is very complicated and cumbersome. This is due to delicate structure of the brain anatomy, especially in the ventricular area, which makes both geometrical modeling and software analysis (e.g., the meshing procedure) very difficult if not impossible. The other drawback of these models is the fact that analysis of the fluid phase might not yield to conversion of the simulation in some portions of the model [13]. Our approach to construct a 2D model from the ventricular system overcomes these problems.

As the results show, the maximum velocity and pressure drop occurring in the pulsatile model is twice the amount in the case of non-pulsatile model. This might be due to increased flow rate during systolic phase of each

cardiac cycle. These results are in accordance with the results derived from CINE MRI and previous results in the literatures [13]. Both maximum velocity and pressure drop occur in aqueduct as the area of the aqueduct is considered to be effective in the case of ventricular fluid dynamics. This is due to its special geometry of small diameter and long length. The average amount of pressure drop in this area is about 0.8Pa which is in accordance with the amount of 1.0Pa reported by Jacobson et al. The diastolic back flow was not seen in these models due to omitting the interaction of surrounding tissue and considering the ventricular walls as a rigid structure. There are more similarities between the results of the pulsatile model and the experimental data due to its resemblance to pusatile nature of CSF flow. Future models considering interaction of the ventricular wall and surrounding structures might indicate a major improvement in recreation of this complex procedure that is the human cerebral fluid hemodynamic.

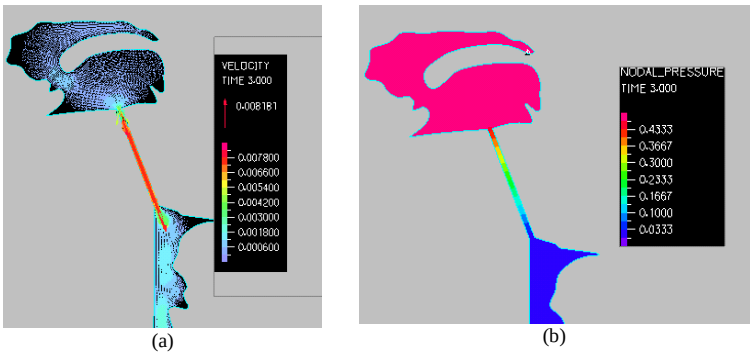

(a) (b)

Fig.2: (a) Velocity vector (b) pressure distribution, in the first person with pulsatile input.

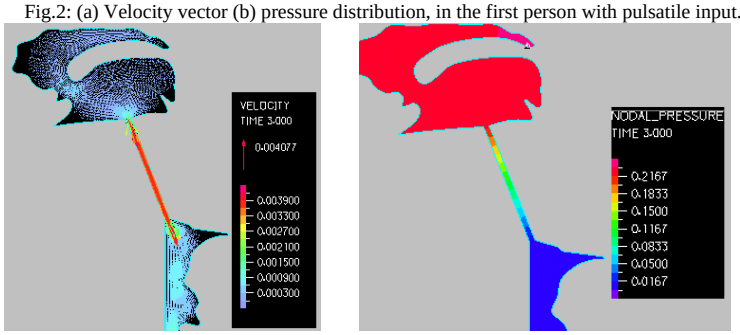

(a) (b)

Fig.3: (a) Velocity vector (b) pressure distribution, in the first person with constant input.

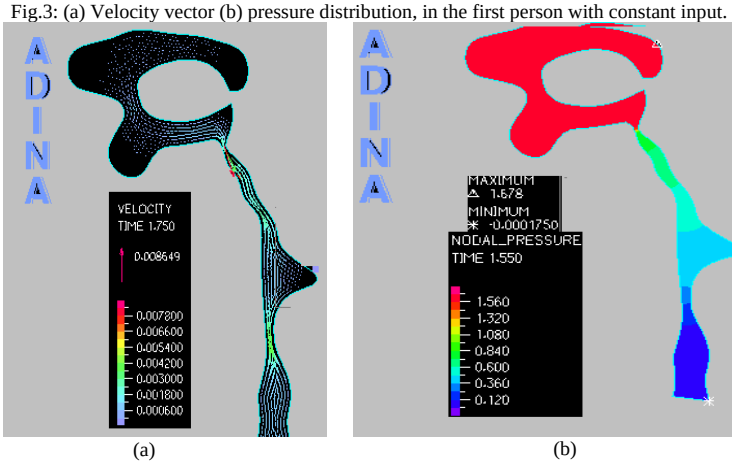

(a) (b)

Fig.4: (a) Velocity vector (b) pressure distribution, in the second person with pulsatile input.

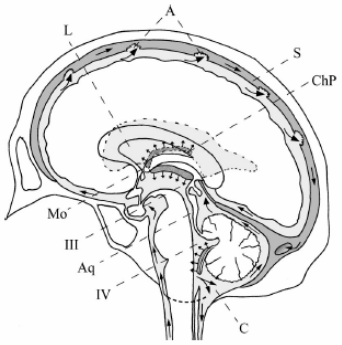

Fig.5: Subarachnoid space, Aq: aqueduct of Sylvius, L: lateral ventricles, III: third ventricle, IV: fourth ventricle [12].

Table 1: Geometrical models, simplicity and conditions comparison.

Simplification	Model
Aqueduct modeling, rigid wall, constant input	Jacobson [2]
Rigid wall, constant input, not modeling subarachnoid space	Aroussi [6]
Modeling unreal volumes, constant input, not modeling SAS	Kurtcuoglu [5]
2D modeling, tissue modeling as intracellular fluid	Linninger [13]

Table 2: Boundary conditions.

Boundary conditions	Output	Input
Surrounded space is considered as rigid wall	From Magendie foramina	CSF flow from third ventricle in the choroid plexus and lateral ventricle
Zero velocity on the wall	ICP= 15mmHg	1- Constant production, q=600 ml/day 2- Pulsatile production, $q_i(t)= q_{bulk}+q_{puls}(t)$

Table 3: Material properties.

Property	Value
Density	$1004-1007\ {}^{kg}/_{m^3}$
Viscosity	0.001Pa.s

Table 4: Velocity and pressure results for two kind of input for the first person.

Parameter	Pulsatile flow	Constant flow	Reports
Velocity in Aqueduct	$8\ {}^{mm}/_{sec}$	$4.5\ {}^{mm}/_{sec}$	$13\ {}^{mm}/_{sec}$ [12] $3.7-7.6\ {}^{mm}/_{sec}$ [12] $23-25\ {}^{mm}/_{sec}$ [12]
Velocity in Magendie foramina	$2.5\ {}^{mm}/_{sec}$	$1\ {}^{mm}/_{sec}$	$2.4-5.6\ {}^{mm}/_{sec}$ [12]
Velocity in Monro	$1\ {}^{mm}/_{sec}$	$1\ {}^{mm}/_{sec}$	$1-3\ {}^{mm}/_{sec}$ [10,12]
Pressure Drop in Aqueduct	0.5Pa	0.2Pa	0.6 – 10Pa [10,12]
Pressure Difference in Ventricle	0.7Pa	0.3Pa	5 – 20Pa [12]

Table 5: Velocity and pressure results for two kinds of input for the second person.

Parameter	Pulsatile flow	Constant flow	Reports
Velocity in Aqueduct	$8\ mm/sec$	$10\ mm/sec$	$3.7-7.6\ mm/sec$ $23-25\ mm/sec$ [12]
Velocity in Magendie foramina	$1\ mm/sec$	$3.2\ mm/sec$	$2.4-5.6\ mm/sec$ [12]
Velocity in Monro	$1\ mm/sec$	$2\ mm/sec$	$1-3\ mm/sec$ [10,12]
Pressure Drop in Aqueduct	0.2Pa	0.2Pa	0.6 –10Pa 11,12]
Pressure Difference in Ventricle	0.3Pa	1.5Pa	5 – 20Pa [11]

5. REFERENCES

[1] Vaeze Mahdavi M.R., Takian, A.H., "Human Anatomy and Physilogy", Shahed University Publication Company, (1997).

[2] Ursino M., "A Mathematical Study of Human Intractranial Hydrodynamics PART1–The Cerebrospinal Fluid Pulse Pressure." Annals of Biomedical Engineering, 16 (1988): 379-401.

[3] Jacobson E., Fletcher D.F., "Computer Modelling of the Cerebrospinal Fluid Flow Dynamics of Aqueduct Stenosis." Medical & Biological Engineering & Computing, 37 (1999): 59-63.

[4] Loth F., Yardimci M.A., et al, "Hydrodynamic Modeling of Cerebrospinal Fluid Motion within the Spinal Cavity." Journal of Biomechanical Engineering—Transactions of the ASME 123, (2001): 71–79.

[5] Kurtcuoglu V., Poulikakos D., et al, "Computational Modeling of the Mechanical Behavior of the Cerebrospinal Fluid System." Journal of Biomechanical Engineering, 127 (2005): 264-269.

[6] Aroussi A., Howden L., et al, "3D Visualisation of Cerebrospinal Fluid Flow Within the Human Central Nervous." Journal of Flow Visualization and Image Processing, 13 (2006): 313-322.

[7] Ammourah S., Aroussi A., et al, "Cerebrospinal Fluid Dynamics in a Simplified Model of the Human Ventricular System." 11th Annual Conference on CFD, Vancouver BC, Canada, (2003). 28-30.

[8] Gibson A., Bayford R. H., et al, "Two-Dimensional Finite Element Modelling of the Neonatal Head." J. Physiology Measurment, 21 (2002): 45–52.

[9] Egnor M., Zheng L., et al, "A Model of Pulsations in Communicating Hydrocephalus." J. Pediatric Neurosurg, 36 (2002): 281–303.

[10] Madsen J.R., Egnor M., "Cerebrospinal Fluid Pulsatility and Hydrocephalus: The Fourth Circulation." Clinial Neurosurgery, 53 (2006): 48-52.

[11] Kurtcuoglu V, Soellinger M., et al, "Computational Investigation of Subject-Specific Cerebrospinal Fluid." J. Biomechanics, 40 (2007): 1235–1245.

[12] Linninger A.A., Xenos M., et al, "Cerebrospinal Fluid Flow in the Normal and Hydrocephalic Human Brain." IEEE Transactions on Biomedical Engineering, 54 (2007): 291-302.

[13] Linninger A.A., Tsakiris C., "Pulsatile Cerebrospinal Fluid Dynamics in the Human Brain." IEEE Transactions on Biomedical Engineering, 52 (2005): 557-565.